Modeling of precipitation processes

Theses of doctoral (Ph.D.) dissertation

Paszkál Papp

Supervisor: **Dr. Dezső Horváth**, *full professor*

Doctoral School of Chemistry

University of Szeged, Department of Physical Chemistry and Materials Science

2024

1 Introduction and Aims

Precipitate formation is an abundant phenomenon both in industrial processes and in nature. Although, active pharmaceutical ingredients, catalysts and paint pigments are made via precipitations, the formation of crystals is not always beneficial, for example in case of limescale or kidney stone formation. In order to achieve greater control over crystallization, and hence to improve the yield or the selectivity in industrial processes, or to decrease the nucleation in case of harmful mineralizations, the deeper understanding of precipitation is inevitable.

Thanks to the increased computational capacity, such reactive heterogeneous systems, besides the experimental investigations, can also be studied via complex theoretical calculations. The modeling of these processes still poses various challenges, since the speed of modern supercomputers is not infinite. The precipitate can be modeled as a concentration field formed by supersaturation, we can describe the solid particles' number and sizes with a density function, or treat their growth and movement individually. The aim of theoretical scientists is to find the equations and methods, which are the most suitable to describe the system.

During my work, I studied precipitation reactions in well-stirred, reaction-diffusion controlled and flow-driven systems with various methods. My aim was to provide theoretical background for experimentally investigated systems, discover the driving force behind physicochemical phenomena, and to calculate data, which is experimentally hard to determine.

The objective of my study was to model the particle distribution and its dynamics in case of well-stirred system, and for that the population balance theory was used. This treatment can be used when vast number of particles are present in the system. In such cases a density function is used to describe the temporal change in particle number and size.

Moreover, I aimed to model Liesegang pattern formation in a reaction-diffusion driven system, where an unusual type of spotted precipitate structure forms. With numerical modeling we wanted to prove that the spotted pattern forms due to the slowing of the reactant's diffusion. Besides that, a numerical model was developed to describe the nucleation, growth and trajectories of the solid particles in a flow-driven system. The model was validated by the simulation of calcium oxalate precipitation in a microfluidic reactor. Furthermore, it was also used to investigate the driving force behind the spatial precipitate separation of copper(II)- and cobalt(II) oxalate in an open surface Hele-Shaw reactor.

2 Modeling

During chemical modeling the aim is to determine the temporal and/or the spatial concentration distribution of the species in the system. In order to achieve this the component mass balance equation

$$\frac{\partial c_i}{\partial t} = \sum_{r=1}^{R} \omega_{i,r} k_r \prod_{j=1}^{N} c_j^{m_{r,j}} + D_i \nabla^2 c_i - \vec{u} \nabla c_i, \tag{1}$$

has to be solved, where D_i the diffusion coefficient of the i-th specimen, $\vec{u}$ is the velocity vector, k_r is the reaction rate coefficient in the r-th reaction, $\omega_{i,r}$ is the stochiometric coefficient and $m_{r,j}$ is the partial order. Depending on the properties of the system, different forms of the mass balance equation should be solved. In a well-stirred system the concentration has only temporal dependence, since the spatial distribution is homogeneous. Therefore, its temporal change is determined by the reaction kinetics, so only the first, kinetic term, is present in the equation. In this case the problem is zero dimensional. If the concentration distribution is inhomogeneous the second, so-called diffusion term appears in Eq. (1). In flow-driven systems the mixing effect of the fluid also needs to be taken into account, which can be done with the third, convective term. Since in this term the velocity vector field is present, it also needs to be calculated. In order to obtain the flow field the Navier–Stokes equation has to be solved

$$\frac{\partial \vec{u}}{\partial t} + (\vec{u} \cdot \nabla)\vec{u} = \nu \nabla^2 \vec{u} - \frac{1}{\rho_0} \nabla p + \frac{\rho}{\rho_0} \vec{g}, \tag{2}$$

where ν is the kinematic viscosity, p is the pressure, $\vec{g}$ is the gravitational acceleration, and ρ is the density. Even in case of isothermal processes the densities of the solutions depend on concentration. In order to model this contribution to the flow the Boussinesq-approximation was used

$$\rho = \rho_0 + \sum_i \rho_i c_i, \tag{3}$$

where ρ_0 is the density of the solvent and $\rho_i = \partial \rho / \partial c_i$. For the modeling of well-stirred and reaction-diffusion systems the `CVODE` integrator module of the `SUNDIALS` software package was used. In case of flow-driven systems, the Navier–Stokes equation was solved with `OpenFoam`, which is a free and open source software for computational fluid dynamics.

3 New Scientific Results

I. *We introduced a new approach to model precipitation reactions based on the temporal evolution of product concentration, from which particle size distribution, their dynamics and specific interfacial energies can be obtained in well-stirred systems [1].*

In order to calculate the particle size distribution, we have to determine the temporal change of an experimentally measured signal which is proportional to the concentration of the precipitate. In this work a previously investigated calcium oxalate precipitation was selected, where the reaction was followed via turbidity measurement. Assuming, that there is a relation, analogous to the Lambert-Beer law, the measured turbidity values can be converted to concentrations. The curves obtained this manner were fitted using the population balance theory coupled with classical nucleation theory. Therefore, as a result the particle size distribution, their dynamics and specific interfacial energies could be obtained (Fig. 1). Experimental particle sizes, determined from scanning electron microscopy images and specific interfacial energies from literature were compared to the outcome of the calculation, and they were in good agreement with each other. The developed model is a general one, therefore it can be used in case of other precipitation processes or experimental setups to determine particle size distributions and their temporal change.

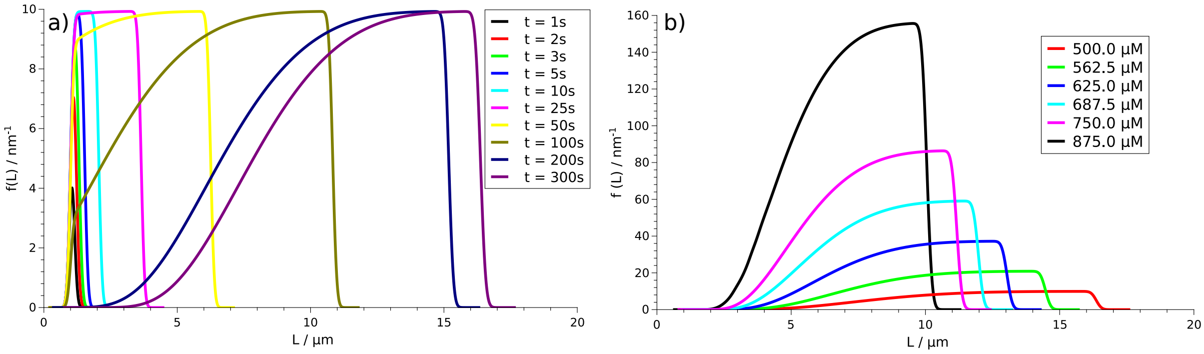

Figure 1: The evolution of particle size distribution in case of $c_{init} = 500\ \mu$M a) and at different initial reactant concentrations in $t = 300$ s b).

II. *With modeling we proved that the cadmium(II) hydroxide precipitate pattern formed in a reaction-diffusion system can be controlled with the binding of hydroxide ions* [5].

Hydroxide ions diffused to a gel containing cadmium(II) ions and a striped pattern formed of cadmium(II) hydroxide precipitate. In a poly(acrylamide-co-methacrylic acid) hydrogel the amount of methacrylic acid was increased, which interacts with the incoming hydroxide ions. The hydroxide ions react with the fixated carboxyl groups in an acid-base equilibrium reaction, therefore the propagation of the reaction front is decreased. In this case the usual striped Liesegang pattern splits and dotty precipitate structure forms. Further increasing the concentration of methacrylic acid in the gel the striped pattern reappears.

In order to describe the Liesegang phenomena the spinodal phase decomposition theory served as a base of our model. During the calculations the Cahn–Hilliard equation was solved, which originates from the Ginzburg–Landau relation and describes the process of spontaneous phase separation. Our results show, that in the absence of binding spotted patterns appear due to the two dimensional thermal perturbation. By the increment of carboxyl groups the velocity of the reaction front decreases, therefore the concentration gradient arising in the direction of propagation will be dominant compared to the thermal noise, which promotes the formation of striped pattern seen in Fig. 2.

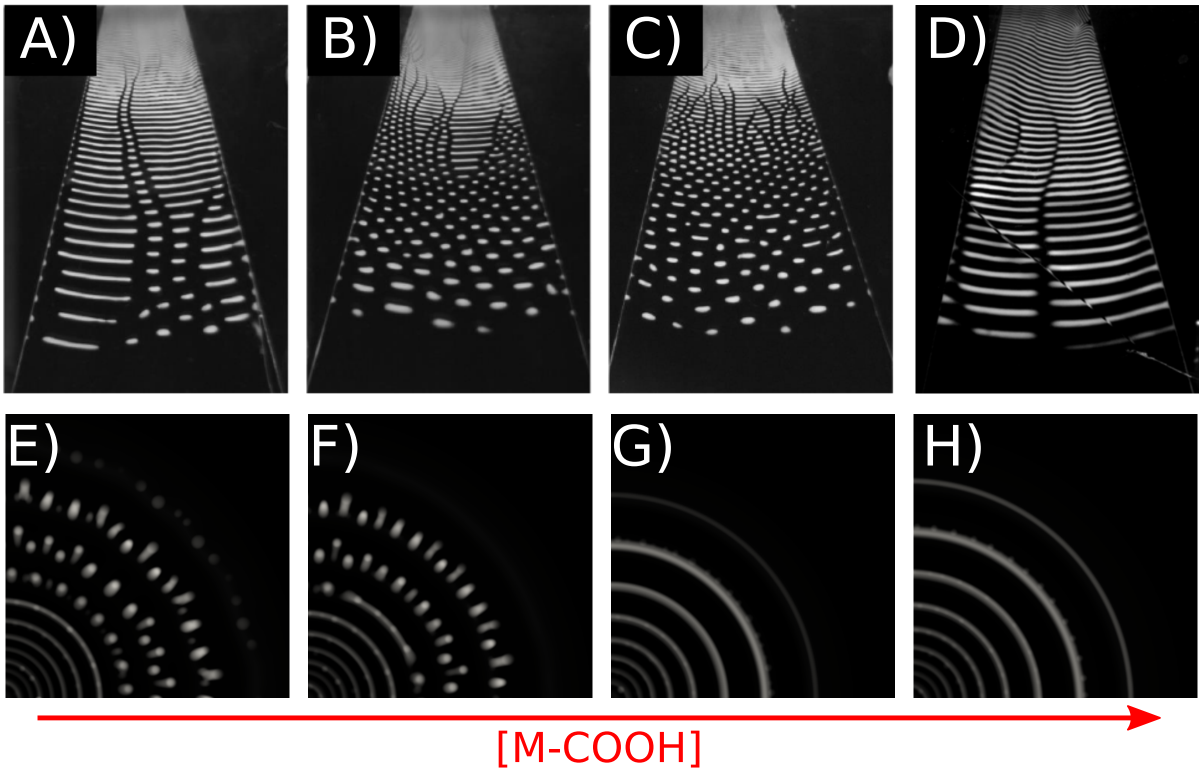

Figure 2: The change in cadmium(II) hydroxide precipitate pattern with increasing methacrylic acid concentration in the experiments (A-D) and in the numerical calculations (E-H).

III. *We created a model which describes the nucleation and the growth of solid particles in a flow-driven system* [4].

In case of flow-driven systems, in order to calculate the temporal change in concentration, which is described by the component balance equation (1), the velocity vector field of the fluid must be known. To obtain the flow field, the Navier–Stokes equation (2) must be solved. The resulting homogeneous concentration (c_i) can be used to calculate the amount of heterogeneous solid phase formed. The rate of precipitation (r_h) can be given as

$$r_h = \left(k_n + k_g \sum_j A_j\right)\left(\prod_i c_i - K_{sp}\right), \tag{4}$$

where k_n and k_g are the rate of nucleation and growth respectively, A_j is the surface of the solid particle and K_{sp} is the solubility product. From Eq. (4) the change in the amount of substance of nucleation (Δn_n) and growth (Δn_g) can be determined in proportion with the reaction rate coefficients

$$\Delta n_n = \frac{k_n}{k_n + k_g \sum_j d_j^2} r_h \Delta t \Delta V, \quad \Delta n_g = \frac{k_g d_j^2}{k_n + k_g \sum_j d_j^2} r_h \Delta t \Delta V.$$

Using the amount of substance obtained this way, we can calculate, based on the

$$1\ \mu\text{m} \leq d_{\text{new}} = \left(\frac{6M\,\Delta n_n}{\rho_p\,\pi}\right)^{1/3},$$

criterion and equation, where ρ_p is the density of the solid particle and M is the molar mass, whether to create a particle in the unit volume at a specific iteration step, or not. Moreover, in case of nucleation the size of the nuclei can also be determined. The size of the j-th particle already present in the volume cell is increased at each iteration step according to

$$d_{\text{new,j}} = \left(d_j^3 + \frac{6M\,\Delta n_g}{\rho_p\,\pi}\frac{d_i^2}{\sum\limits_j d_j^2}\right)^{1/3}$$

equation. The developed model was validated on two flow-driven systems of micrometer and centimeter size ranges.

IV. *We showed that the nucleation positions of the calcium oxalate monohydrate particles sedimented in a microfluidic channel become inhomogeneous with time* [2].

The behavior of calcium oxalate particles was studied, by flowing calcium chloride and sodium oxalate solutions into a microfluidic channel. In order to study the formation of the precipitate its nucleation was investigated with numerical modeling. The spatiotemporal change of the nucleation sites of the sedimented particles was determined and it is shown in Fig. 3. In the beginning of the precipitation the formation of nuclei is homogeneous in the reactor due to high supersaturation. As time progresses, further from the inlet the nucleation of particles decreases, moreover it is limited to the upper parts of the channel. This can be explained by the competitive nature of particle nucleation and growth. Initially the formation of nucleus is dominant in the whole reactor. Later as the particles grow they also sediment, and because of this the nucleation at the lower part of the channel will be suppressed. Since the supersaturation is highest at the confluence of the solutions, particles will appear at the beginning of the reactor but only in the upper regions. However, at other parts of the channel the concentration of the reactants will not be high enough for nuclei formation. Therefore, over time the position of nucleation sites becomes inhomogeneous, since it will be limited to the upper regions close to the beginning of the reactor.

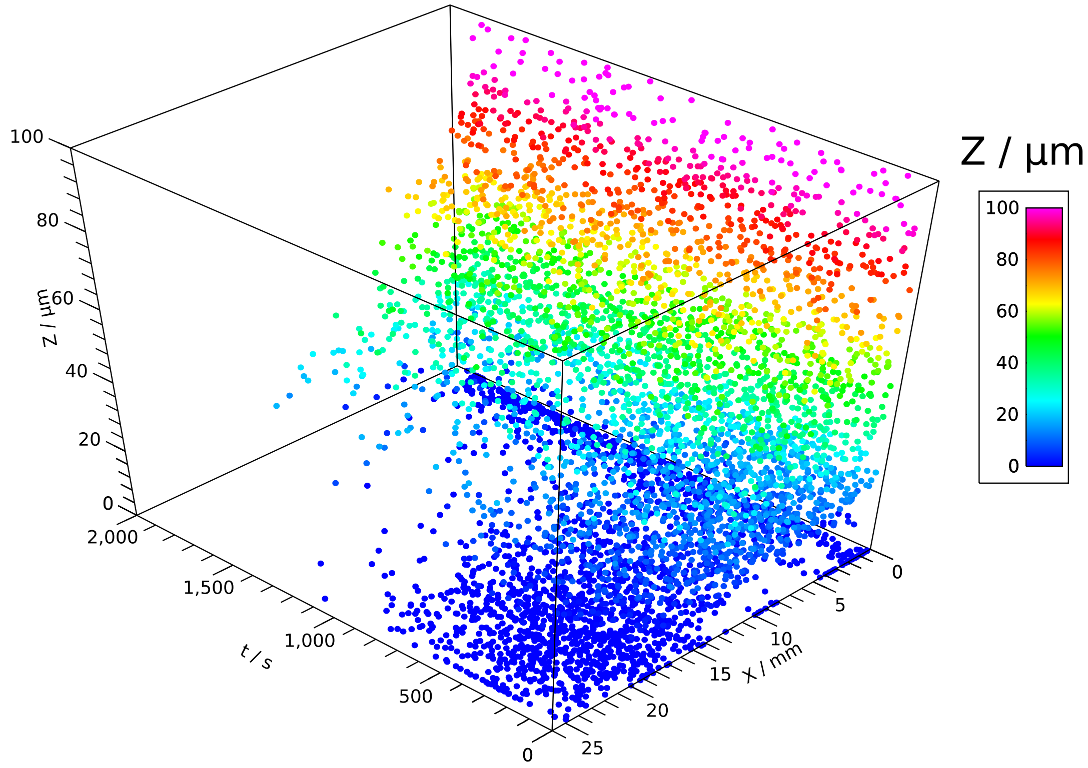

Figure 3: The temporal change of sedimented particles' nucleation sites in the microfluidic reactor.

V. *We showed that the growth of the separately sedimented particles in a microfluidic channel is flow-driven, and the size distribution of the particles leaving the reactor is monodisperse* [4].

Further investigating the behavior of calcium-oxalate particles using the developed model, we could show that besides supersaturation their growth is also influenced by the distance between them. The growth of particles isolated from the others is proportional to $t^{1/3}$, which is shown in Fig. 4 a), therefore their growth is flow-driven. The size of particles sedimented in groups does not change significantly since there is a competition among them. The particles which form further from the bottom of the reactor will drift out of the channel. The size distribution of these particles was determined by modeling. The distribution presented in Fig. 4 b) is highly monodisperse and the polydispersity index is 1.2. The change in dispersity over time is negligible. This can be explained with the nucleation of particles, since it always takes place at the beginning of the reactor, where the supersaturation is high. Due to this, the crystals will spend the same amount of time in the microchannel, and reach similar sizes.

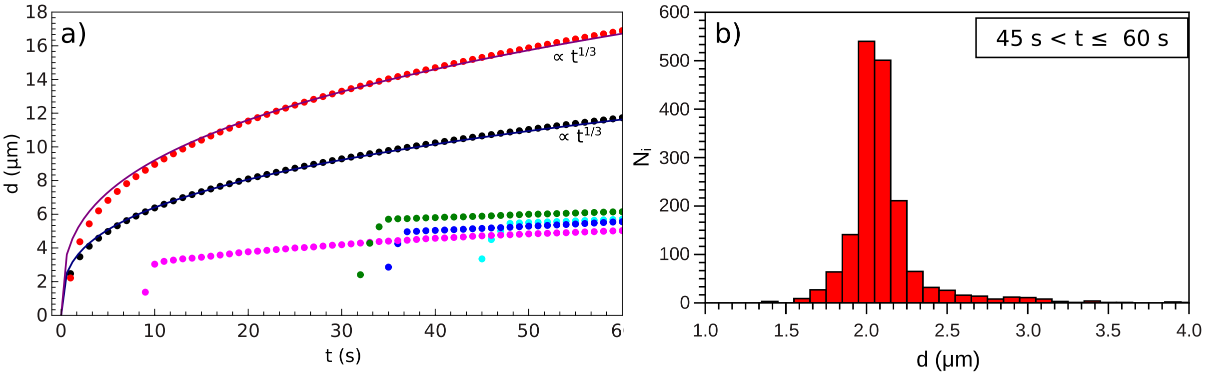

Figure 4: The growth of solid particles a) and the size distribution of particles leaving the reactor b)

VI. *We showed that the spacial precipitate separation of copper(II)- and cobalt(II)-oxalte in a flow-driven system is determined by the complex formation prior to precipitation* [3].

In a well-stirred system, upon mixing cobalt(II)-, copper(II)- and oxalate ions, the cobalt(II)- and copper(II) oxalate precipitates are formed simultaneously, since their solubility products are similar ($pK_{sp,CoOx} = 8{,}58$; $pK_{sp,CuOx} = 8{,}76$). On the contrary in a flow-driven system, when the homogeneous mixture of cobalt(II)- and copper(II) ions is pumped into a reactor containing sodium oxalate, the two precipitates separate from each other spatially. In order to discover the driving force behind this phenomena, we created a model, in which we implemented the following precipitate and complex formation reactions:

$$\begin{aligned}
\mathrm{Co^{2+}_{(aq)}} + \mathrm{C_2O^{2-}_{4\,(aq)}} &\rightleftarrows [\mathrm{CoC_2O_4}]_{(aq)} \rightarrow \underline{\mathrm{CoC_2O_4}}\\
\mathrm{C_2O^{2-}_{4\,(aq)}} + [\mathrm{CoC_2O_4}]_{(aq)} &\rightleftarrows [\mathrm{Co(C_2O_4)_2}]^{2-}_{(aq)}\\
\mathrm{Cu^{2+}_{(aq)}} + \mathrm{C_2O^{2-}_{4\,(aq)}} &\rightleftarrows [\mathrm{CuC_2O_4}]_{(aq)} \rightarrow \underline{\mathrm{CuC_2O_4}}\\
\mathrm{C_2O^{2-}_{4\,(aq)}} + [\mathrm{CuC_2O_4}]_{(aq)} &\rightleftarrows [\mathrm{Cu(C_2O_4)_2}]^{2-}_{(aq)}.
\end{aligned}$$

We managed to simulate the spatial precipitate separation seen in the experiments, which is shown in Fig. 5.

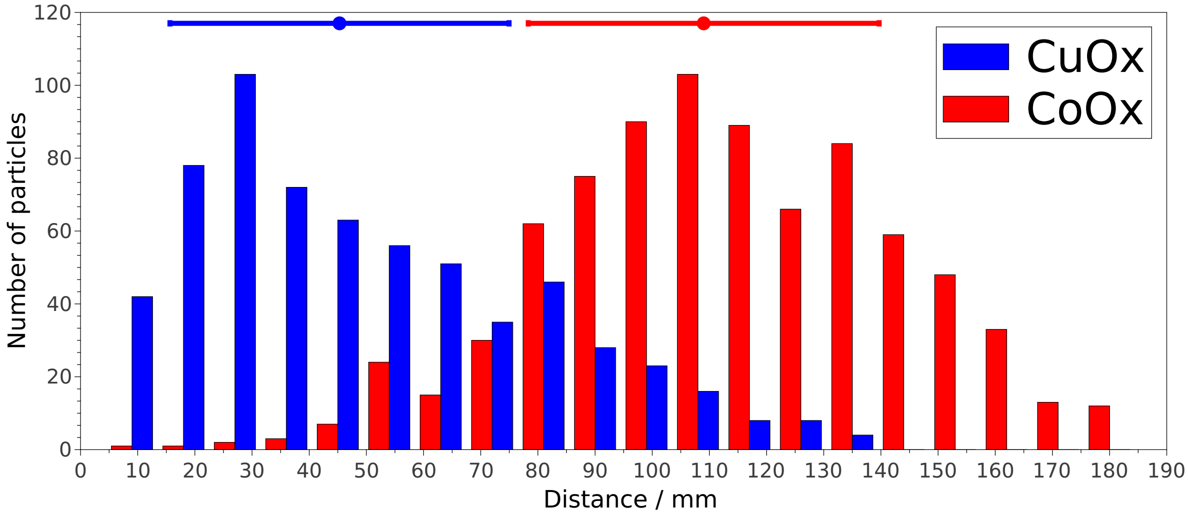

Figure 5: The spatial distribution of the sedimented cobalt(II)- and copper(II) oxalate precipitates. At the x-axis 0 mm is the position of the confluence.

Moreover, we could show from the complex concentration distributions, presented in Fig. 6, that the spatial precipitate separation is caused by the previously formed complexes. Since the complex formation constant of oxalato copper(II) is greater than that of oxalato cobalt(II) ($log_{10}\beta_{CuOx} = 4{,}84, log_{10}\beta_{CoOx} = 3{,}25$), the former forms closer to the

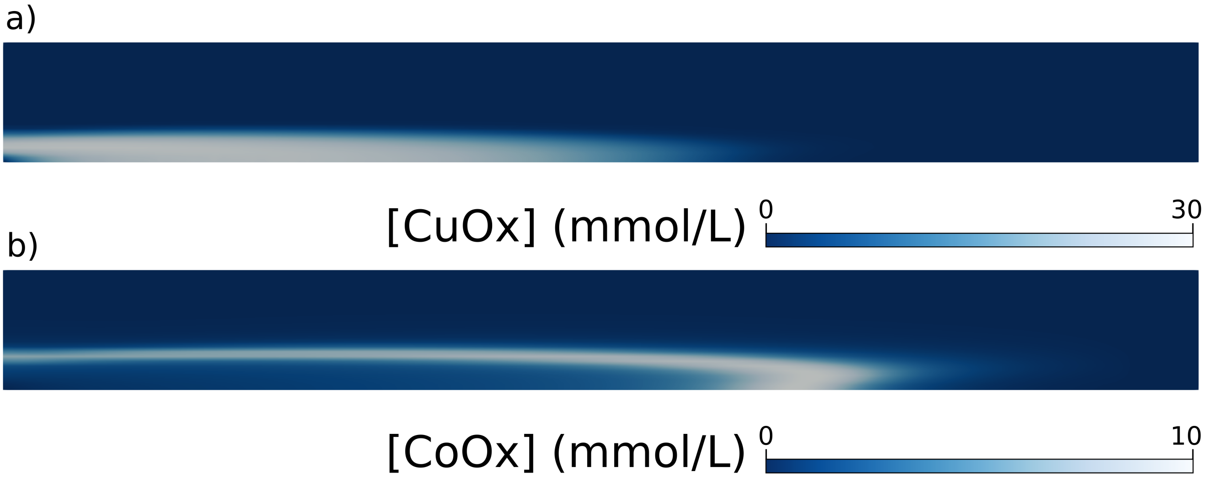

Figure 6: The spatial distribution of oxalato copper(II) (a) and cobalt(II) (b) complexes

bottom of the reactor. Therefor the copper(II) oxalte precipitate, formed from this complex, can sediment closer to the injection point. The oxalato cobalt (II) complex, which is the precursor of the cobalt(II) oxalate precipitate, can only form at the upper regions of the reactor. Due to this the cobalt(II) oxalate solid particles will stay further in the flow, and will sediment spatially later.

4 List of Scientific Publications

4.1 Scientific Publications Related to the Topic of the Dissertation

1. **P. Papp**, Á. Tóth, D. Horváth

   Population mass balance model for precipitation with turbidity measurements

   ACS Omega, **9**, 13412-13417 (2024)

   IF_{2023} = 3.7 (Q2)

2. **P. Papp**, S. Bourg, M. Emmanuel, Á. Tóth, A. Abou-Hassan, D. Horváth

   Spatiotemporal distribution of calcium oxalate crystals in a microchannel

   Cryst. Growth Des., **11**, 8116 (2023)

   IF_{2023} = 3.2 (Q2)

3. **P. Papp**, Á. Tóth, D. Horváth

   Spatial precipitate separation enhanced by complex formation

   Chem. Eng. Sci., **261**, 117955 (2022)

   IF_{2022} = 4.7 (Q1)

4. K. Rakotozandriny, S. Bourg, **P. Papp** Á. Tóth, D. Horváth, I. T. Lucas, F. Babonneau, C. Bonhomme, A. A. Hassan

   Investigating CaOx crystal formation in absence and presence of polyphenols under microfluidic conditions in relation with nephrolithiasis

   Cryst. Growth Des., **20**, 20243-20247 (2020)

   IF_{2020} = 4.076 (Q1)

5. **P. Papp**, B. Bohner, Á. Tóth, D. Horváth

   Fine tuning of pattern selection in the cadmium–hydroxide-system

   J. Chem. Phys., **152**, 094906 (2020)

   IF_{2020} = 3.488 (Q1)

   $\sum$IF =19.164

4.2 Other Scientific Publications

1. **P. Papp**, Á. Tóth, D. Horváth

   PaReDiSo: A reaction-diffusion solver coupled with OpenMPI and CVODE

   Comput. Phys. Commun., **301**, 109193 (2024)

   IF_{2023} = 7.2 (D1)

2. Y. Stergiou, D. M. Escala, **P. Papp**, D. Horváth, M. J. B. Hauser, F. Brau, A. De Wit, Á. Tóth, K. Eckert, K. Schwarzenberg

   Unraveling dispersion and buoyancy dynamics around radial $A + B \rightarrow C$ *reaction fronts: microgravity experiments and numerical simulations*

   npj Microgravity, **10**, 53 (2024)

   IF_{2023} = 4.4 (Q1)

3. Y. Stergiou, **P. Papp**, D. Horváth, Á. Tóth, K. Eckert, K. Schwarzenberg

   Experimental and numerical investigation of a density-driven instability during a horizontal miscible displacement

   Phys. Fluids, **35**, 064112 (2023)

   IF_{2023} = 4.1 (D1)

4. Y. Stergiou, M. J. B. Hauser, A. Comolli, F. Brau, A. De Wit, G. Schuszter, **P. Papp**, D. Horváth, C. Roux, V. Pimienta, K. Eckert, K. Schwarzenberg

   Effects of gravity modulation on the dynamics of a radial $A + B \rightarrow C$ *reaction front*

   Chem. Eng. Sci., **257**, 117703 (2022)

   IF_{2022} = 4.7 (Q1)

5. M. Emmanuel, **P. Papp**, G. Schuszter, A. Deák, L. Janovák, Á. Tóth, D. Horváth

   Nucleation kinetics of lithium phosphate precipitation

   CrystEngComm, **24**, 4447–4453 (2022)

   IF_{2022} = 3.1 (Q2)

6. **P. Papp**, G. Czakó

   Rotational mode specificity in the $F^- + CH_3I\ (v = 0, JK)\ S_N2$ *and proton-transfer reactions*

   J. Phys. Chem. A, **124**, 8943–8948 (2020)

   IF_{2020} = 2.781 (Q2)

7. **P. Papp**, V. Tajti, G. Czakó

   Numerical separation of the front-side attack and double-inversion retention pathways of SN2 reactions

   Chem. Phys. Lett., **755**, 137780 (2020)

   IF_{2020} = 2.328 (Q2)

8. E. Balog, **P. Papp**, Á. Tóth, D. Horváth, G. Schuszter

   The impact of reaction rate on the formation of flow-driven confined precipitate patterns

   Phys. Chem. Chem. Phys., **22**, 13390–13397 (2020)

   $\mathrm{IF}_{2020} = 3.676$ (Q1)

∑IF =32.285
∑∑IF =51.449

5 Lectures

5.1 Lectures Related to the Topic of the Dissertation

1. **Papp Paszkál**, Horváth Dezső

   Csapadékképződési folyamatok modellezése

   Preliminary presentation of dissertation, Reaction Kinetics and Photochemistry Working Group of HSA, 30.05.2024, Balatonvilágos, Hungary

2. **Papp Paszkál**, Tóth Ágota, Horváth Dezső

   Csapadékképződés kinetikai jellemzése populáció-mérleg modellel

   Reaction Kinetics and Photochemistry Working Group of HSA, 09.06.2023, Balatonvilágos, Hungary

3. **Papp Paszkál**, Tóth Ágota, Horváth Dezső

   Spatial precipitate separation enhanced by complex formation

   Japan-Hungarian Workshop, 14.03.2022, Budapest, Hungary

4. **Papp Paszkál**, Tóth Ágota, Horváth Dezső

   Spatial precipitate separation enhanced by complex formation

   COST Chemobrionics Pisa, 06.09.2022, Pisa, Italy

5. **Papp Paszkál**, Tóth Ágota, Horváth Dezső

   Numerical modeling of precipitate formation in a microfluidic system

   GRS Oscillations and Dynamic Instabilities in Chemical Systems, 16.07.2022, Easton, MA, United States

6. **Papp Paszkál**, Tóth Ágota, Horváth Dezső

   Csapadékképződés modellezése folyadékfázisban

   Institutional ÚNKP conference, 03.06.2022, Szeged, Hungary

7. **Papp Paszkál**, Tóth Ágota, Horváth Dezső

   Kémiai reakció és a közegmozgás kölcsönhatásának modellezése szilárd-folyadék rendszerben

   XLIV. Chemistry Lectures, 21.10.2021, Szeged, Hungary

8. **Papp Paszkál**, Tóth Ágota, Horváth Dezső

   Spatial separation of precipitate in reactive media

   2nd Conference on Nonlinearity, 09.10.2021, Belgrade, Serbia

9. **Papp Paszkál**, Tóth Ágota, Horváth Dezső

   Kalcium-oxalát csapadékképződésének modellezése mikrocsatornákban

   Institutional ÚNKP conference, 24.06.2021, Szeged, Hungary

10. **Papp Paszkál**, Tóth Ágota, Horváth Dezső

    Numerical modeling of precipitate formation in microfluidic system

    2nd International Conference on Reaction Kinetics, Mechanisms and Catalysis, 21.05.2021, Budapest, Hungary

11. **Papp Paszkál**, Tóth Ágota, Horváth Dezső

    Csapadékképződés modellezése mikrofluidikás reaktorban

    Reaction Kinetics and Photochemistry Working Group of HSA, 07.11.2019, Mátrafüred, Hungary

12. **Papp Paszkál**, Tóth Ágota, Horváth Dezső

    Csapadékképződés modellezése mikrofluidikás reaktorban

    XLII. Chemistry Lectures, 28.10.2019, Szeged, Hungary

13. **Papp Paszkál**, Tóth Ágota, Horváth Dezső

    Controlling pattern fomration of cadmium-hydroxide system

    Conference on Nonlinearity, 11.10.2019, Belgrade, Serbia

14. **Papp Paszkál**, Tóth Ágota, Horváth Dezső

    Csapadékmintázat képződésének modellezése

    Institutional ÚNKP conference, 21.06.2019, Szeged, Hungary

15. **Papp Paszkál**, Tóth Ágota, Horváth Dezső

    Csapadékmintázat képződésének modellezése

    KeMoMo-QSAR, 06.06.2019, Szeged, Hungary

16. **Papp Paszkál**, Tóth Ágota, Horváth Dezső

    Kadmium-hidroxid csapadékképződés modellezése

    XLI. Chemistry Lectures, 15.10.2018, Szeged, Hungary

17. **Papp Paszkál**, Tóth Ágota, Horváth Dezső

    Kadmium-hidroxid csapadékképződés modellezése

    Reaction Kinetics and Photochemistry Working Group of HSA, 24.05.2018, Balatonalmádi, Hungary

6 Posters

6.1 Poster Presentations Related to the Topic of the Dissertation

1. **Papp Paszkál**, Tóth Ágota, Horváth Dezső

   Modeling the kinetics of spatiotemporal precipitation

   12th International Conference on Chemical Kinetics, 26.06.2023, Hefei, China

2. **Papp Paszkál**, Tóth Ágota, Horváth Dezső

   Spatial precipitate separation enhanced by complex formation

   COST Chemobrionics Pisa, 06.09.2022, Pisa, Italy

3. **Papp Paszkál**, Tóth Ágota, Horváth Dezső

   Spatial precipitate separation enhanced by complex formation

   GRC Oscillations and Dynamic Instabilities in Chemical Systems, 20.07.2022, Easton, MA, United States

4. **Papp Paszkál**, Tóth Ágota, Horváth Dezső

   Spatial separation of precipitates in reactive media

   Understanding Crystallisation: Faraday Discussion, 28.03.2022, York, United Kingdom

6.2 Other Poster Presentations

1. **Papp Paszkál**, Stergiou Yorgos, Schuszter Gábor, Tóth Ágota, Eckert Kerstin, Schwarzenberger Karin, Horváth Dezső

   Radiális reakciófront terjedése súlytalanságban

   Hungarian Space Research Forum, 03.05.2023, Sopron, Hungary

MTMT identification number: 10074723